Arab J Geosci (2015) 8:8741–8752
DOI 10.1007/s12517-015-1814-7

ORIGINAL PAPER

Structure of the Yanbu suture zone in Northwest Saudi Arabia inferred from aeromagnetic and seismological data

Mokbel Al-Harbi · Elkhedr Ibrahim · Abdullah Al-Amri · Kamal Abdelrahman · EssamAbd El-Motaal · Meinrat O. Andreae

Received: 23 September 2014 / Accepted: 20 January 2015 / Published online: 4 February 2015

Abstract The present work focuses on a study of the Yanbu suture zone and related ophiolites using aeromagnetic and seismological data. The interpretation of aeromagnetic data indicates that NW–SE- and NE–SW-trending structural faults dominate the study area. These faults coincide with narrow and elongated magnetic highs, possibly caused by intrusions emplaced along the faults. The NE trend is dissected by cross-cutting NW-trending faults in some places. The NE-oriented suture zone is marked by short-wavelength high magnetic anomalies associated with ultramafic rocks (ophiolites) and is divided by the NW-oriented left-lateral Najid faulting (Qazaz shear zone) into two shifted alignments. This implies that deep-seated regional trends govern to a large extent the location and extension of the ophiolite exposures. There is a clear correlation between land earthquakes and the interpreted magnetic structures, where the majority of earthquake epicenters lie on or close to the interpreted major faults. A clear concentration of earthquakes is observed where the NE-trending faults cross the Red Sea NNW-trending faults. Here, two separate aftershock clusters occur to the north of Yanbu City, indicating the reactivation of the pre-existing Precambrian NE-trending transform fault,which crosses two parallel NNW-trending faults that have been injected by Cenozoic volcanics during the Cenozoic rifting of the Red Sea. These results indicate that the seismotectonics of the study area is strongly related to the geodynamic rifting processes acting in the Red Sea, where the relative movement between African and Arabian plates resulted in several series of normal and transform faults that run parallel and cross the Red Sea, respectively.

Keywords Rifting · Fault trends · Ophiolites · Seismotectonics

M. Al-Harbi · E. Ibrahim · A. Al-Amri · K. Abdelrahman (✉) · E. El-Motaal · M. O. Andreae
Geology and Geophysics Department, College of Science, King Saud University, Riyadh, Kingdom of Saudi Arabia
e-mail: ka_rahmaneg@yahoo.com

M. O. Andreae
Biogeochemistry Department, Max Planck Institute for Chemistry, Mainz, Germany

E. Ibrahim
Geology Department, Faculty of Science, Mansoura University, Mansoura, Egypt

K. Abdelrahman
Seismology Department, National Research Institute of Astronomy & Geophysics, Helwan, Cairo, Egypt

E. El-Motaal
Geology Department, Faculty of Science, Al-Azhar University, Cairo, Egypt

Introduction

The Arabian shield, as a part of the Arabian–Nubian shield, is made up mostly of juvenile Neoproterozoic crust but locally contains tectonically intercalated Archean and Paleoproterozoic rocks (Stern and Johnson 2010). It displays amalgamated tectonostratigraphic terranes of Tonian (1000–850 Ma) and Cryogenian (850–650 Ma) volcanic and plutonic rocks (Johnson et al. 2003, 2011; Johnson and Kattan 2012). This led to the formation of the 40–100-km thick lithosphere of the Arabian shield (Mooney et al. 1985; Altherr et al. 1990; Camp and Roobol 1992; Sandvol et al. 1998; Hansen et al. 2007). North- and northeast-trending sutures have been postulated between the distinct terranes since the mid-1970s (Al-Shanti and Mitchell 1976) on the basis of ophiolite- and serpentinite-decorated shear zones (Johnson et al. 2004). The NE-oriented Yanbu suture is situated between the Midyan and

Hijaz terranes on the northwestern side of the Arabian shield (Fig. 1). The ophiolites of the Arabian shield range in age from ~690 to ~870 Ma and have a mean age of ~780 Ma, which may approximate the onset of terrane accretion (Stern et al. 2004). The Arabian shield has an older Neoproterozoic (>800 Ma) core of accreted intra-oceanic arcs in the west, flanked by younger arc terranes (>740 Ma) to the east and north (Stoeser and Frost 2006). Thus, there appears to be a progressive trend towards younger ages of oceanic arcs eastwards across the Arabian shield, but the significance of this trend is not yet clear. A suturing event along the eastern margin of the Afif terrane is marked by the occurrence of the Halabanophiolite at ~680–670 Ma (Al-Saleh et al. 1998).

Suture zones are significant pieces of evidence preserved within the continental crust marking the places of continental collision that led to accretion-related orogenic tectonic deformation. Commonly accepted indicators of continental collision include dismembered ophiolites, ultra-high pressure metamorphic rocks, igneous and metamorphic rocks with reset isotopic systems, and post-collisional granites. Suture zones are ductile shear zones resulting from thrusting along convergent plate boundaries, and their width ranges from a few hundred meters to tens of kilometers (Coward et al. 1982). They mark the sites of subducted oceanic lithosphere and consequent welding of continental masses (Dewey 1977). Gneiss belts and domes are locally associated with the suture zones in the Arabian shield. They are broadly aligned along a NW-oriented system of ductile to brittle shear/fault zones, referred to as the "Najd Corridor"' (Fritz et al. 1996), which most workers correlate with the Najd fault system in the Arabian shield. The study area displays ophiolitic exposures dissected and dislocated by the left-lateral faults of the NW-oriented Najd fault system (Fig. 2). Different high-grade foliated rocks along the NW-oriented Qazaz–Ajjaj sinistral shear zone and the Hamadat gneiss belt include hornblende gneiss, tonalite gneiss, granodiorite gneiss, and granite gneiss. Moreover, strongly deformed volcanic and sedimentary rocks include quartzofeldspathic schist, amphibolite and amphibole schist, migmatite of alternating quartzofeldspathic and amphibole schist, garnet- and kyanite-bearing schist, and schistose volcanic rocks (Johnson et al. 2011).

Our study region is the Yanbu area on the northwestern side of Saudi Arabia, bounded by latitudes 23° and 27° N and longitudes 36° and 40° E (Fig. 2). This area is located between the Midyan and Hijaz tectonostratigraphic terranes in the northwestern part of the Neoproterozoic Arabian shield (Fig. 1).

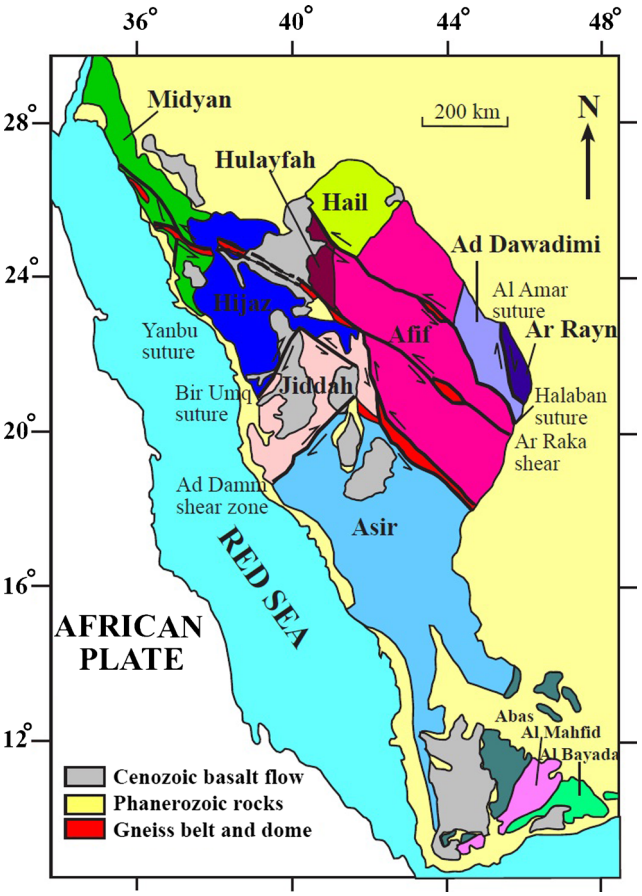

Fig. 1 Sketch map showing the tectonostratigraphic terranes of the Arabian shield and their boundaries

Geologic setting

The Arabian shield is a part of the Arabian–Nubian shield that existed before the Red Sea rift and consists primarily of Neoproterozoic juvenile crust. It represents an area of suturing between East and West Gondwana before the Paleozoic (Johnson et al. 2013). It is made up of several distinct tectonostratigraphic terranes resulting from the accretion of numerous, mainly inter-oceanic, island arcs along ophiolite-lined suture zones and gneissic fault zones (Windley et al. 1996; Al-Saleh et al. 1998; Cox et al. 2012; Eyal et al. 2014). It was formed between 900 Ma and 550 Ma, when the Mozambique Ocean closed (Stern et al. 1990). These terranes are separated by major, mainly N–S- and NE–S-trending, suture zones marked by serpentinized ultramafic rocks (ophiolites and tectonic slices) and by major NW-oriented shears of the Najd fault system. The extent and amount of displacement or deformation associated with the Najd fault system are controversial (Sultan et al. 1988; Andre 1989; Sengör and Natalin 1996; Smith et al. 1998; Kusky and Matsah 2000, 2003; Johnson et al. 2004). This Najd-type structure is an en-echelon set of shear zones that extends from the Qazaz–Ajjaj shear zone in the northwest to the ArRikah shear zone in the southeast (Fig. 2). Initial movements on the ArRikah fault followed deposition of the Murdama group (650–625 Ma), and subsequent movements followed emplacement of 611 Ma granitoids (Johnson et al. 2011).

Movements along the Qazaz–Ajjaj shear zone are constrained to between ~635 Ma and ~573 Ma (Calvez et al. 1984; Kennedy et al. 2010). This was bracketed by cataclastically deformed granite with an inferred reset Rb–Sr age of 630 ± 19 Ma and the emplacement of an undeformed, post-shearing lamprophyre dike at 573 Ma, which cuts paragneiss and schist along the shear zone (Johnson et al. 2011). The Ajjaj shear zone crosscuts the N-oriented Hanabiq right-lateral shear zone (Fig. 2). Alternatively, the Hanabiq may form a "zipper" shear with the Ajjaj shear zone (Passchier 2010). Close to the Red Sea, the Najd fault pattern is spatially associated with negative magnetic lineaments that are subparallel to the coast and mark major Cenozoic dikes.

The Yanbu suture zone is characterized by ophiolite rocks (Fig. 2) distributed in the area from JabalEss to Jabal Al Wasq (JabalEss–Wadi Al Hwanet and the Jabal Al Wasq–Al-Ays belts). The JabalEss-Al Hwanet and Jabal Al Wasq–Al-Ays belts contain the complete ophiolitic successions particularly at JabalEss (Al-Shanti and Roobol 1979; Al-Shanti and Gass 1983). Ten locations of ophiolite outcrops have been observed. These are the West Al-Ays, Al-Ays, Jabal Al Wasq, Jabal Al-Ays, BirFuqayer, JabalEss, WadiWajh, JabalOweined, WadiHawanet, and WadiEssophiolites. The ophioliticallochthonous rocks are emplaced unconformably with a tectonic thrust contact over volcanosedimentary rocks and are intruded by late to post-tectonic plutons.

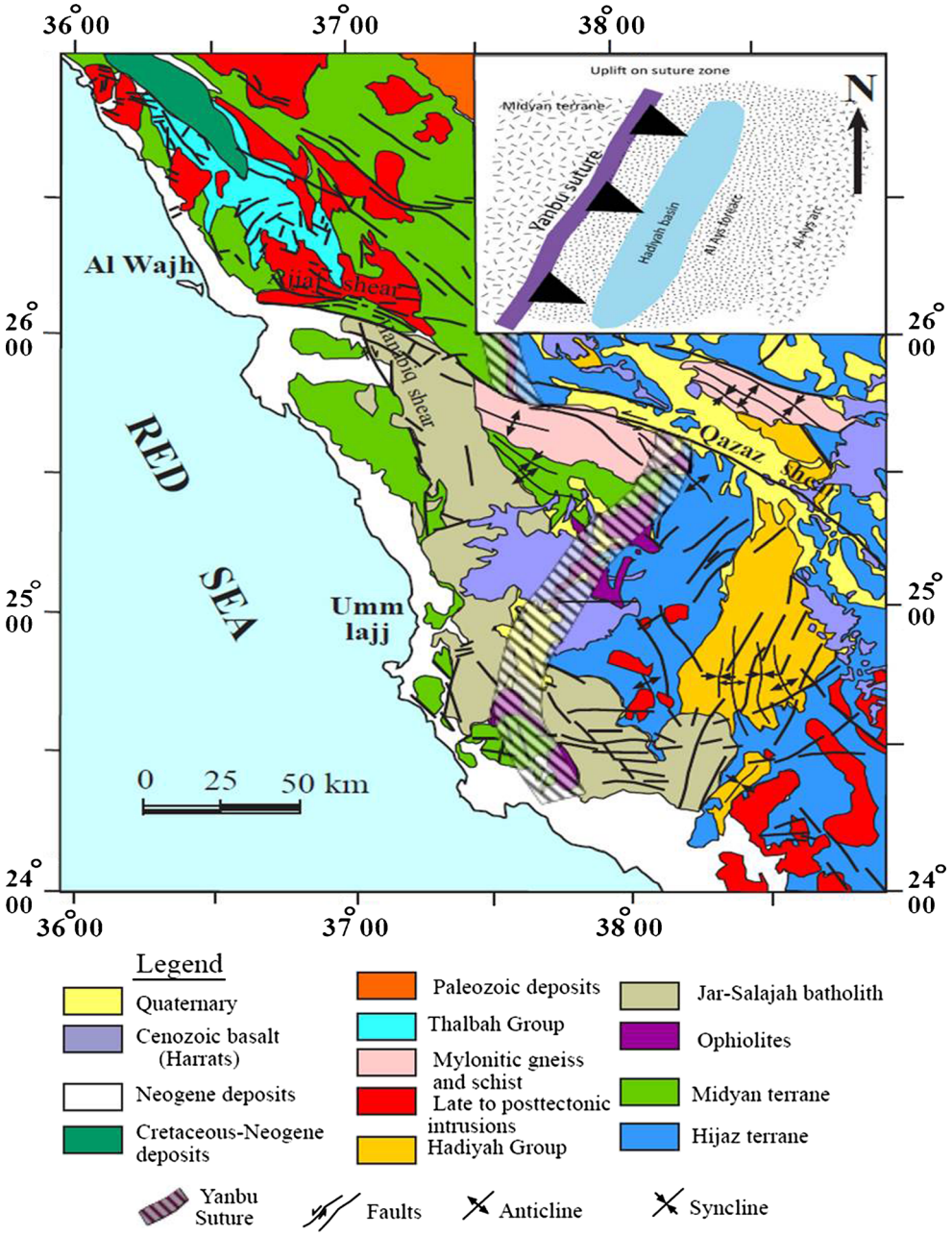

Fig. 2 Geological map of the Yanbu suture area, from Johnson et al. (2013), schematically shows the tectonic setting of the suture zone

Belts and domes of gneiss are locally exposed along early to middle Cryogenian suture zones (Fig. 3), including the Hulayfah–Ad Dafina–Ruwah fault zone (Johnson and Kattan 2001), the Bi'rUmq-Nakasib suture (Johnson et al. 2003; Hargrove 2006), and the Nabitah fault zone (Stoeser and Stacey 1988). The Kirsh, An Nakhil, Wajiyah, and Ajjaj-Hamadat-Qazaz gneiss belts and domes are associated with a 1300-km-long en-echelon NW-oriented Qazaz–ArRikah shear zone (Al-Saleh 2010; Andresen et al. 2010). This shear zone extends across the entire Arabian shield and continues into the Nubian shield in Egypt as the Meatiq, El Sibai, and Hafafit gneiss domes and associated Najd faults (Sturchio et al. 1983a, b; El Ramly et al. 1984; Stern et al. 1989; Greiling et al. 1994; Fritz et al. 1996; Fowler and Osman 2009). The gneisses of the Arabian shield reflect brittle–ductile deformation and intervening greenschist-amphibolite metamorphism with brittle deformation along the Najd faults. This reveals several P/T amphibolite to-greenschist transitions along the strike of the Najd faults (Johnson et al. 2011). Ductile deformation continued until at least 575 Ma, the protolith age of granite gneiss on the northern margin of the Ajjaj shear zone, but ceased prior to the intrusion of undeformed 573 Ma lamprophyre dikes (Kennedy et al. 2011). The Ajjaj shear zone and steeply dipping Hamadat gneiss belt are strongly foliated and lineated with lineations plunging gently SE and NW. L–S fabrics predominate but L-tectonites are locally present. Poles to foliation in the Hamadat gneiss (Fig. 3) define a broad girdle, compatible with the map-scale anticlinorium that has been mapped in the gneiss, and broad antiformal structures are found in part of the Qazaz gneiss (Johnson et al 2011).

Several post-tectonic mafic, felsic, and composite mafic–felsic dikes have been dated, including lamprophyre dikes that intrude the Ajjaj shear zone in the Midyanterrane (573 ± 6 Ma;

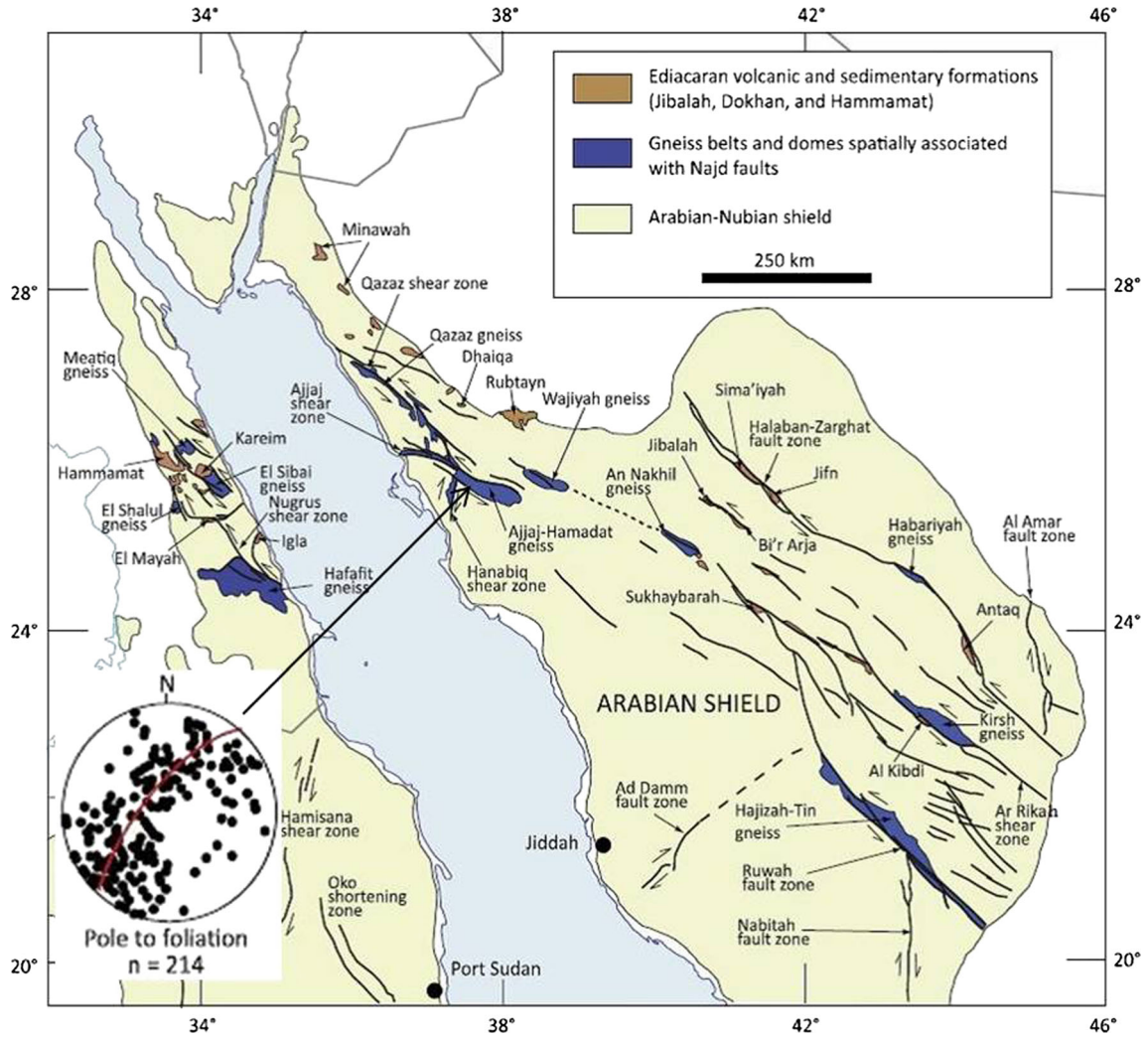

Fig. 3 Spatial and genetic relationships between the northwest-trending Qazaz and Ajjaj shear zones and the Qazaz and Ajjaj-Hamadat gneisses; *inset* shows poles to foliation in the Hamadat gneiss (after Johnson et al. 2011)

Kennedy et al. 2011). They represent some of the youngest Neoproterozoic rocks in the study area and cross cut most other rocks and structures.

Aeromagnetic data processing and interpretation

A high-resolution aeromagnetic anomaly map of the study area is used here for mapping and delineating the structural elements, such as faults and shear zones, between the Neoproterozoicterranes, as well as dikes that trace the Yanbu suture zone and their associated ophiolite exposures. For this purpose, the aeromagnetic data were first subjected to various transformations to enhance the data resolution such as reduction to the pole, Butterworth filtering, and preparing the tilt derivative and first vertical derivative maps. The total field magnetic anomaly (TMI) map of the study area (Fig. 4) was reduced to the pole (RTP) to overcome the bipolarity of the magnetic data (Fig. 5).

The most prominent feature appearing in Fig. 5 are the disconnected, nearly circular and strong magnetic anomalies exceeding 500 nT that are aligned across the north to northeast direction and surrounded by weak magnetic anomalies. The stronger anomalies are correlated with ophiolite exposures distributed along the Yanbu suture zone from JabalEss on the north to Jabal Al Wasq to the south (Fig. 5). The ophiolite outcrops are composed of mantle peridotite, layered gabbro, dike complex, and pillow basalt (Al-Shanti and Gass 1983). Their dominant mafic and ultramafic composition is clearly reflected by the strong magnetic anomalies, whereas the surrounding relatively low and broad wavelength magnetic anomalies are correlated to the granite and meta-sedimentary units. Further, the magnetic anomalies associated with the ophiolite belt are dissected into two parts and displaced by the left-lateral NW-oriented Najd fault. This fault system mostly coincides with the Qazaz shear zone (GSZ, Fig. 5). These ophiolitic magnetic anomalies are bounded to the southeast by disconnected and nearly circular high magnetic anomalies lined mainly in the N–S and NE–SW direction. These anomalies could be interpreted as serpentinized ultramafic rocks plutons (Fig. 5).

The first vertical derivative map prepared from TMI using Fourier transformation (Fig. 6) presents the higher spatial frequencies in the data due to features such as faults, dikes or geological contacts, and as such can yield information about structures that may not be clear enough in the TMI or RTP plots. Faults in the exposed basement, particularly the Najd fault system (GSZ; Fig. 5) coincide with the narrow and elongated magnetic highs possibly caused by intrusions emplaced along the faults. This shear zone apparently extends across the entire Arabian shield and continues into other areas of the Nubian shield (El Ramly et al. 1984; Stern et al. 1989; Greiling et al. 1994; Fowler and Osman 2009; Fig. 3). To the northwest of the study area, there are elongated, high magnetic anomalies extending in the WNW direction. These

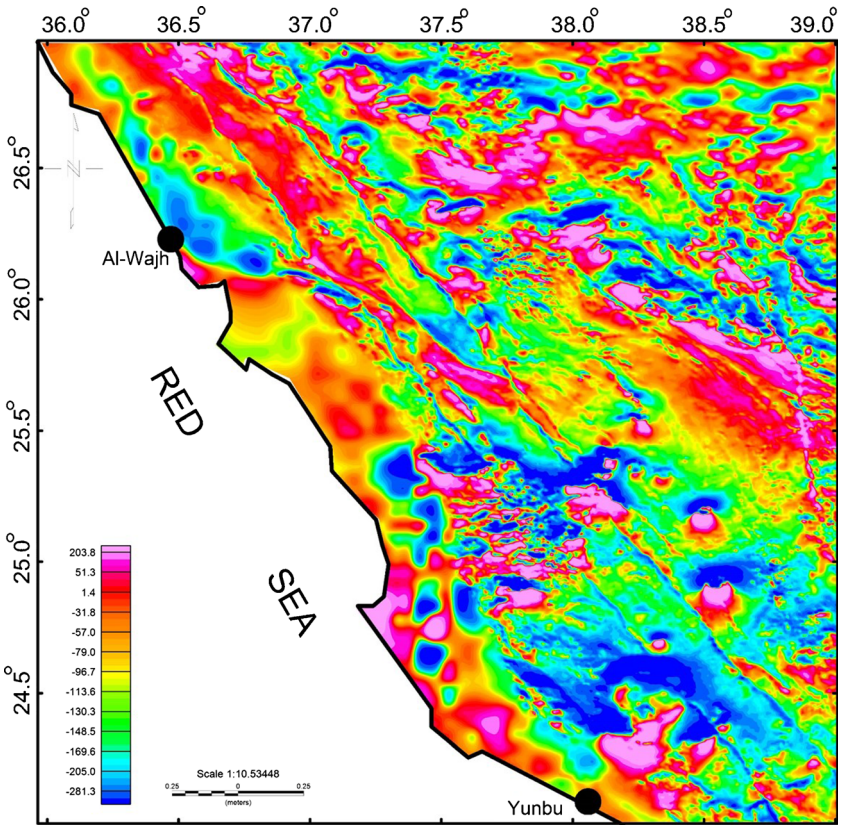

Fig. 4 Total field magnetic intensity map for the study area

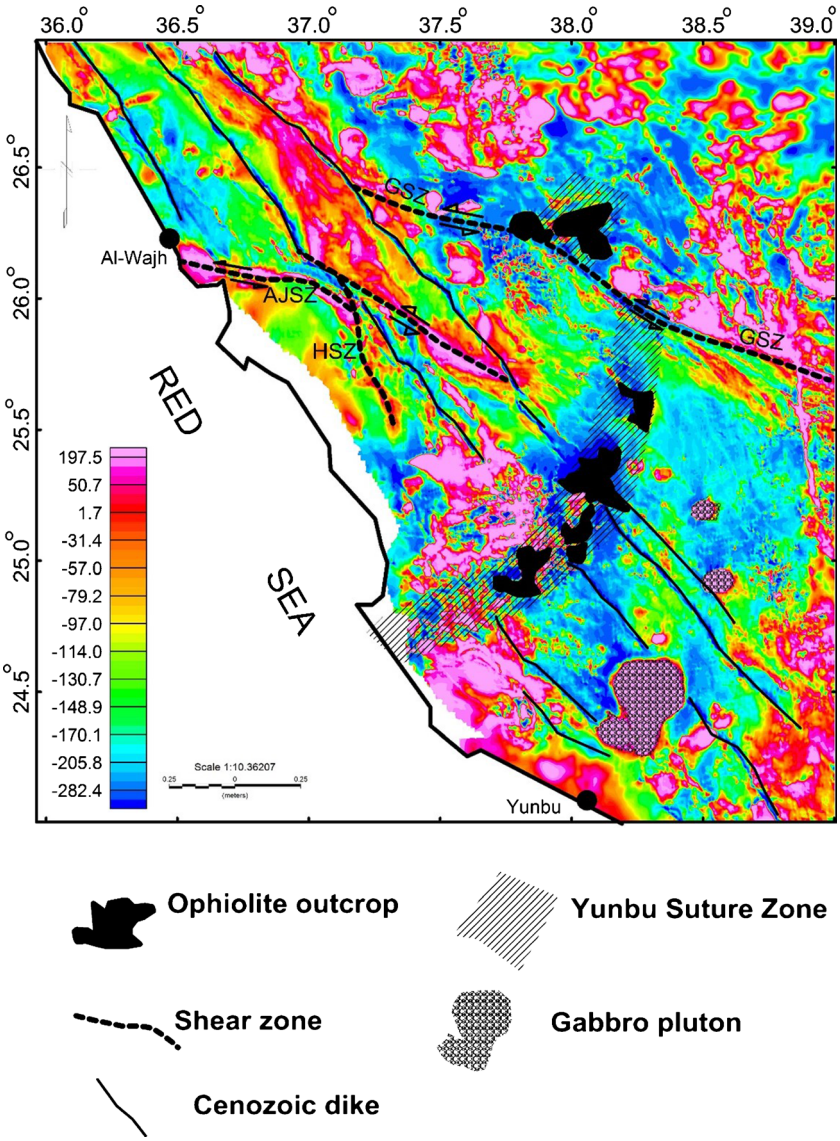

Fig. 5 Reduced-to-the-pole magnetic intensity map for the study area. *GSZ* Gazaz shear zone, *AJSZ* Ajjaj shear zone, *HSZ* Hanabiq shear zone, and *LVF* Lunayyir volcanics field

anomalies are correlated with the mafic, felsic, and composite mafic–felsic dikes that intruded the Ajjaj shear zone (AJSZ) in the Midyan terrane (Kennedy et al. 2011; Fig. 5). The Ajjaj shear zone crosscuts the N-oriented Hanabiq right-lateral shear zone (HSZ) (Fig. 5). Interestingly, there is a conspicuous change in the direction of this fault zone,which becomes curvilinear when it gets closer to the Red Sea coast. This may indicate a fault drag that probably represents a fairly recent movement on the WNW-striking Ajjaj shear zone.

Negative magnetic lineaments that are seen running subparallel to the Red Sea coast probably mark major Cenozoic basaltic dikes. Such dikes are expected to show positive magnetic anomalies (Fig. 6). However, the presence of these intense linear negative magnetic anomalies is probably due to remnant magnetization in the direction reverse from the present-day magnetic field, as known to be characteristic of the Tertiary (Ibrahim et al. 2000; Al-Amri and Fnais 2010).

The magnetic anomalies in the study area are complex because of the heterogeneous, short-wavelength, and high-intensity anomalies interspersed with areas of broad-wavelength anomalies, prominent lineaments, and discrete circular anomalies. This heterogeneity is related to the different exposed rock units: the study area is covered mainly by the Al-Ays and Hadiyah groups that consist of volcanic and sedimentary formations, interspersed in some localities with granodiorite, granite, and mafic and/or felsic plutons. In addition, the volcanic and extrusive basalts in Harrat fields produce regions of heterogeneous high-intensity anomalies in the area. This heterogeneity could mask the subsurface deep structure. Hence, the deep structural interpretation of the magnetic data is attempted here using the regional magnetic anomalies after removing the effects of the surface basalt flows. For this purpose, the RTP data were separated into long-wavelength regional (deep) and short-wavelength residual

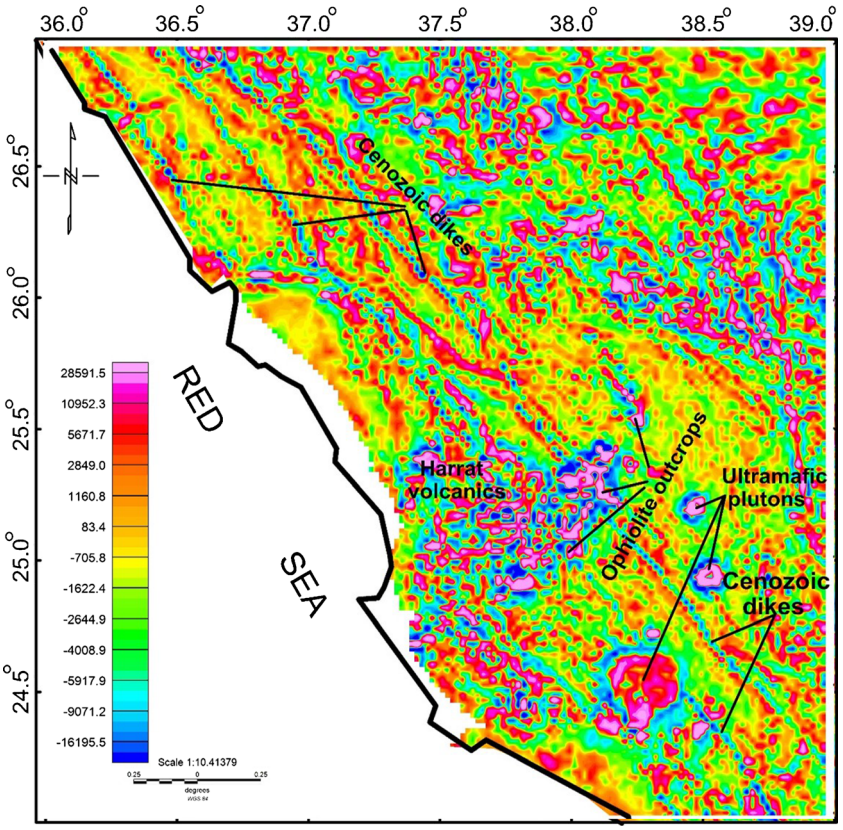

Fig. 6 First vertical derivative map of the aeromagnetic anomalies for the study area

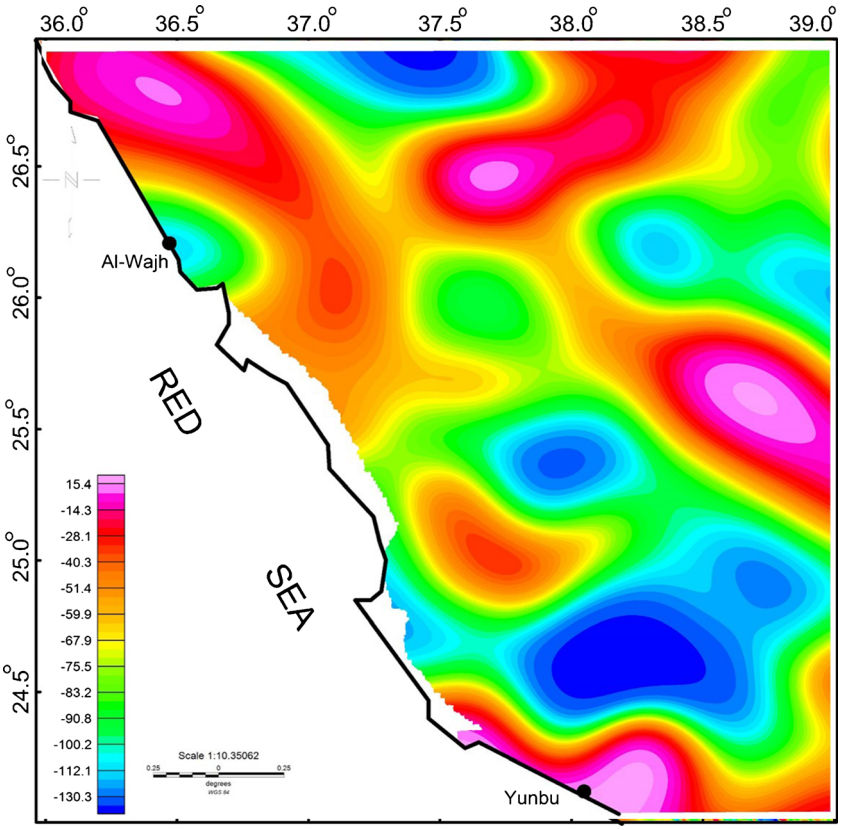

Fig. 7 Regional magnetic anomaly map of the study area

(shallow) components through application of the Butterworth filtering technique. This filter is preferred to band-pass or high-low pass filters in order to overcome the ringing effects (Pawlowski and Hansen 1990).

The regional magnetic map (Fig. 7) shows that two major faulting systems affect the study area, namely, NW–SE and NE–SW fault systems. It is clear also that the NE structure is dissected by cross-cut NW-trending faults that disfigure and truncate the NE structures. Areas with thick sedimentary successions around the contact between the Midyan and Hijaz terranes are represented by areas of low-relief, broad-wavelength anomalies (Fig. 7). To the southeast of the interpreted ophiolite belt, this low broad anomaly is correlated to Hadiyah basin, which is filled with thick sedimentary formations. The areas of moderately intense anomalies reflect a sequence of metasedimentary rocks and granitic plutons. The tilt derivative map (TDR) (Fig. 8) was next prepared from the TMI map in order to identify magnetic lineaments representing the structural trends underlying the study area (Verduzco et al. 2004). Using the TDR anomaly map, it is possible to identify dominant regional structural trends that are otherwise difficult to detect clearly on the total magnetic anomaly map. The zero crossing of the TDR is close to the edge of the structure, so by applying a threshold of 0.0 and plotting the "zero-contour", it is possible to signify the magnetic lineaments. Bodies with positive susceptibility contrast are shown in red and blue color, which indicate significantly decreased magnetization. The TDR map generally confirms the dominance of the NW–SE and NE–SW tectonic trends. The northeast structural trend is seen to be dissected by cross-cutting northwest-trending faults in places, suggesting their age relationship. This further implies that the deep-seated regional trends govern to a large extent the location and extension of the ophiolite exposures.

Seismotectonics

To evaluate the earthquake activity in the study area, an earthquake catalogue for the period 1900–2012 was compiled from the following data sources: (1) two regional catalogues (Ambraseys 1988; Ambraseys et al. 1994), (2) the Seismic Studies Center (SSC) of King Saud University, (3) the Saudi National Seismographic Network (SNSN) of King Abdul-Aziz University for Science and Technology, and (4) the Saudi Geological Survey (SGS). Then, these collected data were merged and correlated with the international earthquake data centers, where earthquake data are precisely analyzed, as follows: (1) on-line bulletin of the International Seismological Center (ISC), (2) on-line bulletin of the United States Geological Survey (USGS), which includes information from the Preliminary Determination of Epicenters (PDE) provided by

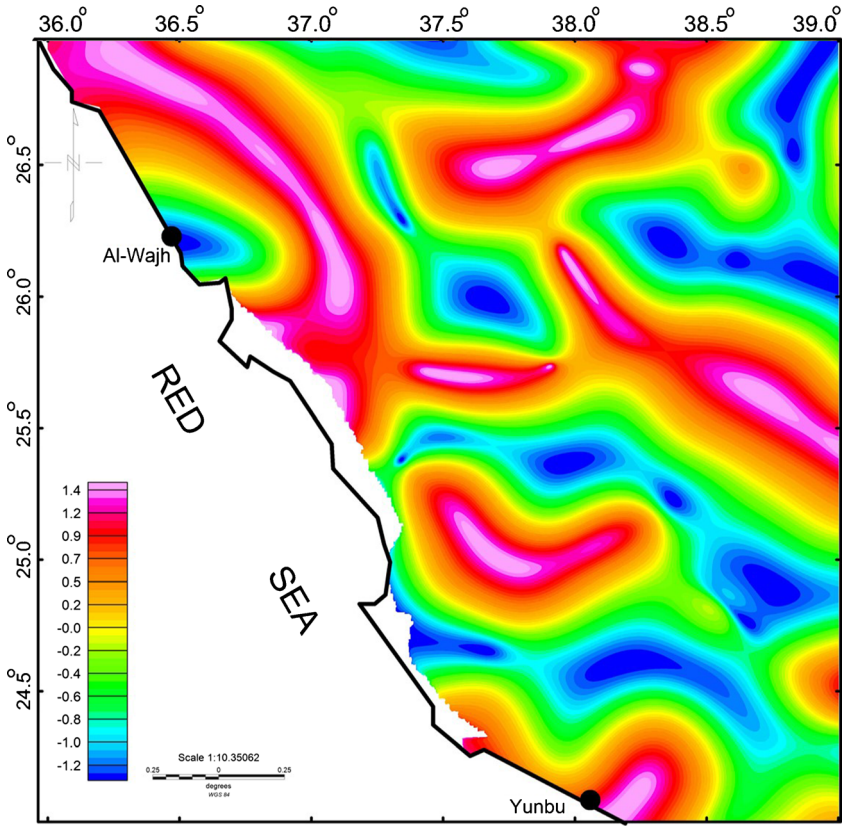

Fig. 8 Tilt derivative map prepared from the TMI map of the study area

the National Earthquake Information Center (NEIC), and (3) on-line bulletin of the European Mediterranean Seismological Center (EMSC). This process was designed to ensure the reliability of the earthquake data sources. Duplicate events were eliminated. Furthermore, foreshock and aftershock sequences were removed from the catalogue using the windowing procedure proposed by Gardner and Knopoff (1974). Many of the finally selected earthquakes had been reported using different types of magnitudes; these were converted and unified into body-wave magnitude (M_b) according to Ambraseys and Bommer (1990), Ambraseys and Free (1997), and Al-Amri et al. (1998). The reported earthquakes were found to have magnitudes in the range of $3 \leq M_b \leq 6.9$.

Finally, the compiled earthquake catalogue was overlaid on the structurally interpreted map of the Yanbu area to construct the seismotectonic map of the study area (Fig. 9). This figure indicates that the land earthquake activity in the Arabian shield appears to be low relative to the Red Sea axial trend, where the majority of earthquakes are concentrated along the spreading zone of the Red Sea. This concentration is seen where the NE-trending transform fault bisects the spreading zone. However, this concentration is not uniformly distributed but occurs in clusters along the rift axis. The occurrence of earthquakes and active volcanism along the Red Sea axial trough indicates the present-day rifting (El-Isa and Al Shanti 1989). In 1121 AD, a damaging earthquake originated in the

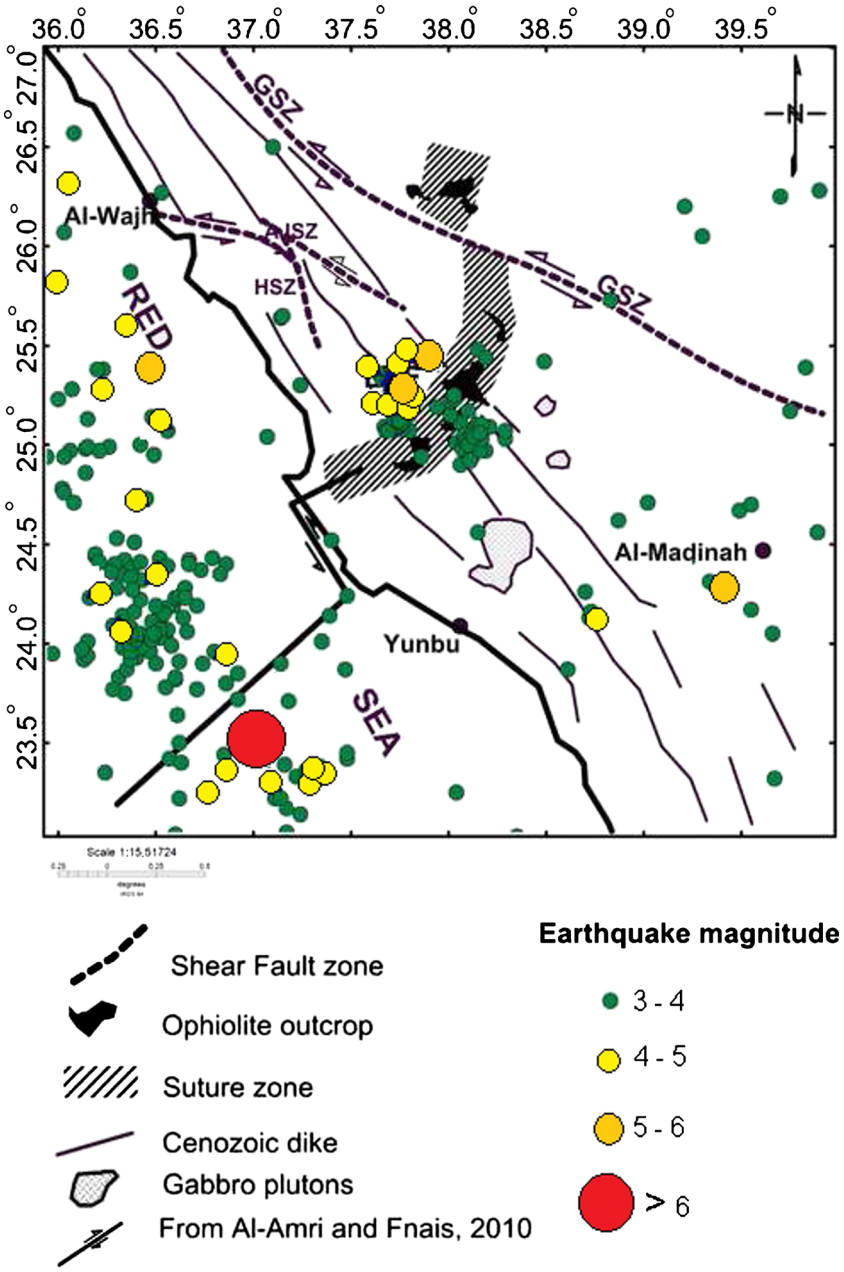

Fig. 9 Seismotectonic map of the Yanbu area

main Red Sea trough (southwest of Yanbu City) with magnitude M_s= 6.8 (Ambraseys et al. 1994). It was strongly felt over a wide area, where damaging effects were reported to relatively long-period structures located about 330 km apart (e.g. Mecca and Al-Madinah). This event was located on the NE–SW-trending transform fault in the Yanbu area, where a maximum recorded intensity of VI was recorded at Sharm Yanbu. The distribution of the aftershocks shows two adjacent clusters, one aligned NW–SE and the other oriented NE–SW. These trends are correlated well with the direction of transform faults crossing the Red Sea and offsetting the Median trench and NW–SE spreading axis of the Red Sea. Alignment of epicenters along the northeast trend near latitude 24° N could indicate that this fault extends northeastward inland as far as the extension of the interpreted Yanbu suture zone that is associated with the ophiolite exposures.

Most land earthquakes are oriented NW to NNW within the Arabian shield. The 1256 AD strong historical earthquake of AlMadinah was definitely a land volcanic earthquake. The 1122 and 1256 AD strong historical earthquake events correlated with the volcanic activity in the Madinah area (El-Isa and Al Shanti 1989). The 1256 AD earthquake of Al Madinah was the largest of a swarm type that experienced ground shaking (Ambraseys 1988) and was accompanied by volcanic activity. Recently, the Yanbu area was struck by a moderate (M_w = 5.7) earthquake on 19 May 2009, which occurred at Harrat Lunayyir (Ash Shaqah), about 120 km north of Yanbu City (Al-Amri and Fnais 2010).

The distribution of the aftershocks from this earthquake shows two separate clusters that are aligned in a NNW direction to the north of Yanbu City. These clusters are correlated with NE-trending faults that are controlled mainly by older pre-existing Precambrian faults and were reactivated during the Tertiary by the NNW-trending Red Sea faults that were injected with Cenozoic volcanics during the rifting of the Red Sea. On 27 August 2009, a felt earthquake (M_b 4.0) occurred in the Badr area (24.11° N and 38.8° E), approximately 50 km from the Red Sea. The focal mechanism of the Badr earthquake indicates a normal faulting mechanism. The location of this earthquake is very close to the NW–SE-trending Najd faults.

Conclusions

Our results indicate that the seismotectonic setting of the study area is strongly related to the geodynamic rifting processes acting in the Red Sea, where the relative movement between the African and Arabian plates resulted in several series of normal and transform faults that run parallel and across the Red Sea, respectively. Some of the transform faults extend inland over tens or hundreds of kilometers (Al Shanti 1966). The NE-oriented Yanbusuture zone is marked by short-wavelength magnetic anomalies associated with ultramafic rocks (ophiolites) and is offset by the NW-oriented left-lateral Najid faulting (Qazaz shear zone). The NW–SE- and NE–SW-trending fault systems dominate the study area. The northeast structural trend is seen to be dissected by cross-cutting northwest-trending faults in some places. This implies that deep-seated regional trends govern to a large extent the location and extension of the ophiolite exposures. Clear concentrations of seismological activity are noticed where the NE-trending faults cross the NW-trending fault system that indicates the present-day rejuvenation of the Tertiary tectonic trends. There is a clear correlation between land earthquakes and tectonics, where the majority of earthquake epicenters lie on or close to the major faults (e.g., the GSZ, HSZ, and AJSZ faults). A great number of earthquakes are located along the NE suture zone that seems to be a continuation of a major NE-oriented transform fault. To the north of Yanbu City, the aftershocks of recent earthquakes are distributed into two separate clusters that are aligned in the NNW (Red Sea) direction. These clusters are correlated with the reactivation of the pre-existing Precambrian NE-trending transform fault and its crossing of two parallel NNW-trending faults that have been injected by Cenozoic volcanics during the Cenozoic rifting of the Red Sea. These results indicate a good correlation between the distribution of earthquake epicenters and the general tectonics of the area.

Acknowledgments The authors would like to extend their sincere appreciation to the Deanship of Scientific Research at King Saud University for funding this research group (No. RG -1435-035).

References

Al Shanti AM (1966) Oolitic iron-ore deposits in Wadi Fatima between Leddah and Mecca, Saudi Arabia. Saudi Arabian Dir. Gen. Min. Resources Bull., 2, 51p

Al-Amri A, Fnais M (2010) Seismo-volcanic investigation of 2009 earthquake swarms at Harrat Lunayyir (Ash Shaqah). International Journal of Earth Sciences and Engineering, Western Saudi Arabia

Al-Amri A, Punsalan B, Uy E (1998) Spatial distribution of the seismicity parameters in the Red Sea regions. J Asian Earth Sci 16:557–563

Al-Saleh AM (2010) The Kirsh gneiss dome: an extensional metamorphic core complex from the SE Arabian shield. Arab J Geosci. doi: 10.1007/s12517-0101-0179-1

Al-Saleh AM, Boyle AP, Mussett AE (1998) Metamorphism and 40Ar/39Ar dating of the Halabanophiolite and associated units: evidence for two-stage orogenesis in the eastern Arabian shield. J Geol Soc Lond 155:165–175

Al-Shanti AM, Gass IG (1983) The upper Proterozoic ophiolite mélange zones of the easternmost Arabian shield. J Geol Soc Lond 140:867–876

Al-Shanti AMS, Mitchell AHG (1976) Late Precambrian subduction and collision in the Al Amar–Idsas region, Kingdom of Saudi Arabia. Tectonophysics 30:T41–T47

Al-Shanti M, Roobol MJ (1979) A Late Proterozoic ophiolite complex at JabalEss in northern Saudi Arabia. Nature (London) 279:488–491

Altherr R, Henjes-Kunst F, Puchelt H, Baumann A (1990) Volcanic activity in the Red Sea axial trough—evidence for a large mantle diapir. Tectonophysics 150:121–133

Ambraseys A (1988) Seismicity of Saudi Arabia and adjacent areas. Report 88/11, ESEE, Imperial Coll. Sci. Tech., 88/11, London

Ambraseys NN, Bommer JJ (1990) Uniform magnitude re-evaluation for strong motion database of Europe. Eur Earthq Eng 4(2):3–16

Ambraseys NN, Free MW (1997) Surface-wave magnitude calibration for European region earthquakes. J Earthq Eng 1(1):1–22

Ambraseys NN, Melville CP, Adams RD (1994) The seismicity of Egypt, Arabia and the Red Sea: a historical review. Cambridge University Press, Cambridge, 181P

Andre CG (1989) Evidence for phanerozoic reactivation of the Najd fault system in AVHRR, TM, and SPOT images of Central Arabia. Photogramm Eng Remote Sensing 55:1129–1136

Andresen A, Augland LE, Boghdady GY, Lundmark AM, Elnady OM, Hassan MA (2010) Structural constraints on the evolution of the Meatiq gneiss domes (Egypt), East-African Orogen. J Afr Earth Sci 57:413–422

Calvez JY, Alsac C, Delfour J, Kemp J, Pellaton C (1984) Geological evolution of western, central, and eastern parts of the northern Precambrian Shield, Kingdom of Saudi Arabia. King Abdulaziz University, Jiddah, Faculty of Earth Science Bulletin 6, 24–48

Camp V, Roobol M (1992) Upwelling asthenosphere beneath western Arabia and its regional implications. J Geophys Res 97:15255–15271

Coward MP, Jan MQ, Rex D, Tarney J, Thirlwall MF, Windley BF (1982) Geo-tectonic framework of the Himalaya of N Pakistan. J Geol Soc Lond 139:299–308

Cox G, Lewis CJ, Collins AS, Nettle D, Halverson GP, Foden J, Kattan F, Jourdan F (2012) Ediacaran Terrane accretion in the Arabian Nubian shield. Gondwana Res 21:341–352

Dewey JF (1977) Suture zone complexities: a review. In: McElhinny, M.W. (Ed.) The past distribution of continents. *Tectonophysics*, vol. 40, pp. 53–67

El Ramly MF, Greiling R, Kroner A, Rashwan AA (1984) On the tectonic evolution of the Wadi Hafafit area and environs, Eastern Desert of Egypt. King Abdulaziz University, Jiddah, Bulletin of the Faculty of Earth Sciences 6, 114–126.e

El-Isa ZH, Al Shanti A (1989) Seismicity and tectonic of the Red Sea and western Arabia. Geophys J 97:449–457

Eyal M, Be'eri-Shlevin Y, Eyal Y, Whitehouse MJ, Litvinovsky B (2014) Three successive Proterozoic island arcs in the Northern Arabian–Nubian shield: evidence from SIMS U–Pb dating of zircon. Gondwana Res 25:338–357

Fowler TJ, Osman AF (2009) Gneiss-cored interference dome associated with two phases of late Pan-African thrusting in the Central Eastern Desert, Egypt. Precambrian Res 108:17–43

Fritz H, Wallbrecher E, Khudeir AA, Abu El Ela F, Dallmeyer DR (1996) Formation of Neoproterozoic metamorphic core complexes during oblique convergence (Eastern Desert, Egypt). J Afr Earth Sci 23:311–329

Gardner JK, Knopoff L (1974) Is the sequence of earthquakes in Southern California, with aftershocks removed, Poissonian? Bull Seismol Soc Am 64(5):1363–1367

Greiling RO, Abdeen MM, Dardir AA, El-Akhal H, El-Ramly MF, Kamal El-Din GM, Osman AF, Rashwan AA, Rice AHN, Sadek MF (1994) A structural synthesis of the Proterozoic Arabian–Nubian shield in Egypt. Geol Rundsch 83:484–501

Hansen SE, Rodgers AJ, Schwartz SY, Al-Amri AMS (2007) Imaging ruptured lithosphere beneath the Red Sea and Arabian Peninsula. Earth Planet Sci Lett 259:256–265

Hargrove US (2006) Crustal evolution of the Neoproterozoic Bi'rUmq suture zone, Kingdom of Saudi Arabia. Geochronological, Isotopic, and Geochemical Constraints. Unpublished Ph.D. thesis, University of Texas at Dallas, 343 p

Ibrahim EH, Odah H, El Agami N, Abu Elenen M (2000) Palaeomagnetic and geologic investigations into some volcanic rocks, southern Sinai, and the rifting of the Gulf of Suez. Tectonophysics 321:343–358

Johnson PR, Kattan FH (2001) Oblique sinistraltranspression in the Arabian shield: the timing and kinematics of a Neoproterozoic suture zone. Precambrian Res 107:117–138

Johnson PR, Kattan FH (2012) The geology of the Saudi Arabian shield. Saudi Geological Survey, Jiddah, pp 1–479

Johnson PR, Abdelsalam MG, Stern RJ (2003) The Bi'rUmq–Nakasib suture zone in the Arabian–Nubian shield: a key to understanding crustal growth in the East African orogen. Gondwana Res 6:523–530

Johnson PR, Kattan FK, Al-Saleh AM (2004) Neoproterozoic ophiolites in the Arabian shield: field relations and structure. In: Kusky TM (ed) Precambrian ophiolites and related rocks, Developments in Precambrian geology, vol. 13. Elsevier, Amsterdam, pp 129–162

Johnson PR, Andresen A, Collins AS, Fowler AR, Fritz H, Ghebreab W, Kusky T, Stern RJ (2011) Late Cryogenian–Ediacaran history of the Arabian–Nubian shield: a review of depositional, plutonic, structural, and tectonic events in the closing stages of the northern East African orogen. J Afr Earth Sci 61:167–232

Johnson PR, Halverson GP, Kusky TM, Stern RJ, Pease V (2013) Volcanosedimentary basins in the Arabian–Nubian shield: markers of repeated exhumation and denudation in a Neoproterozoic accretionary orogen. Geosciences 3:389–445

Kennedy A, Kozdroj W, Kattan FH, Kodzroj MZ, Johnson PR (2010) SHRIMP Geochronology in the Arabian shield (MidyanTerrane, AfifTerrane, Ad DawadimiTerrane) and Nubian shield (Central Eastern Desert), part IV. Data acquisition 2008. Saudi Geological Survey Open-File Report SGS-OF-2010-10, 101p

Kennedy A, Kozdroj W, Johnson PR, Kattan FH (2011) SHRIMP geochronology in the Northern Arabian shield. Part III. Data acquisition 2006. Saudi Geological Survey Open-File Report SGS-OF-2007-9

Kusky TM, Matsah MI (2000) Evolution of a Neoproterozoic dextral pull-apart Basin (Jifn Basin), NE Arabian shield: relationships to the Halaban-Zarghat (Najd) Fault system and the closure of the Mozambique Ocean. Geological Society of America, Annual Meeting 2000

Kusky T, Matsah M (2003) Neoproterozoic dextral faulting on the Najd fault system, Saudi Arabia, preceded sinistral faulting and escape tectonics related to closure of the Mozambique Ocean. In: Yoshida M, Windley BF, Dasgupta S, Powell C (eds) Proterozoic East Gondwana: supercontinent assembly and breakup, vol. 206. Geological Society. Special Publication, London, pp 327–361

Mooney W, Gettings M, Blank H, Healy J (1985) Saudi Arabian seismic refraction profile: a travel time interpretation of crustal and upper mantle structure. Tectonophysics 111:173–246

Passchier C (2010) The Al Wajhshear zone system, NW Saudi Arabia. In: Pease, V., Kadi, K.A., Kozdroj, W. (Eds.) JEBEL project. October 2009 field excursion to the MidyanTerrane, Kingdom of Saudi Arabia with reports on research by participants of the JEBEL Project. Saudi Geological Survey Technical Report SGS-TR-2010-2, pp. 76–77

Pawlowski RS, Hansen RO (1990) Gravity anomaly separation by Wiener filtering. Geophysics 55:532–548

Sandvol E, Seber D, Barazangi M, Vernon F, Mellors R, Al-Amri A (1998) Lithospheric seismic velocity discontinuities beneath the Arabian shield. Geophys Res Lett 25:2873–2876

Sengör AMC, Natalin BA (1996) Paleotectonics of Asia: fragment of a synthesis. In: Yin A, Harrison TM (eds) The tectonics of Asia. Cambridge University Press, New York, pp 486–640

Smith M, O'Conner E, Nasr BB (1998) Transpressional flower structures and escape tectonics: a new look at the Pan-African collision in the

Eastern Desert, Egypt. In: Greiling RO (ed) Workshop on the Pan-African of Northern Africa–Arabia. Geologisch-Palaeontologiches Institut, Ruprecht-KarlsUniversitaet, Heidelberg, October 22–23

Stern RJ, Johnson PR (2010) Continental lithosphere of the Arabian plate: a geologic, petrologic, and geophysical synthesis. Earth Sci Rev 101:29–67

Stern RJ, Kröner A, Manton WI, Reischmann T, Mansour M, Hussein IM (1989) Geochronology of the late Precambrian Hamisana shear zone, Red Sea Hills, Sudan and Egypt. J Geol Soc Lond 146:1017–1029

Stern RJ, Nielsen KC, Best E, Sultan M, Arvidson RE, Kröner A (1990) Orientation of Late Precambrian sutures in the Arabian–Nubian shield. Geology 18:1103–1106

Stern RJ, Johnson PJ, Kröner A, Yibas B (2004) Neoproterozoic ophiolites of the Arabian–Nubian shield. In: Kusky T (ed) Precambrian ophiolites. Elsevier, Amsterdam, pp 95–128

Stoeser DB, Frost CD (2006) Nd, Pb, Sr, and O isotopic characteristics of Saudi Arabian shield terranes. Chem Geol 226:163–188

Stoeser DB, Stacey JS (1988) Evolution, U–Pb geochronology, and isotope geology of the Pan-African Nabitahorogenic belt of the Saudi Arabian shield. In: El-Gaby S, Greiling RO (eds) The Pan-African belt of NE African and adjacent areas. Friedrich, Viewig and Sohn, Braunschweig, pp 227–288

Sturchio NC, Sultan M, Batiza R (1983a) Geology and origin of Meatiq Dome, Egypt: a Precambrian metamorphic core complex? Geology 11:72–76

Sturchio NC, Sultan M, Sylvester P, Batiza R, Hedge C, El Shazly EM, Abdel-Maguid A (1983b) Geology, age, and origin of the Meatiq dome—implications for the Precambrian stratigraphy and tectonic evolution of the Eastern Desert of Egypt. King Abdulaziz University, Faculty of Earth Sciences Bulletin 6, 127–143

Sultan M, Arvidson RE, Duncan IJ, Stern R, El Kaliouby B (1988) Extension of the Najd fault system from Saudi Arabia to the central Eastern Desert of Egypt based on integrated field and Landsat observations. Tectonics 7:1291–1306

Verduzco B, Fairhead JD, Green CM, MacKenzie C (2004) New insights into magnetic derivatives for structural mapping. Lead Edge 23: 116–119

Windley BF, Whitehouse MJ, Ba-Bttat MAO (1996) Early Precambrian gneiss terranes and Pan-African island arcs in Yemen: crustal accretion of the eastern Arabian shield. Geology 24:131–134